# Combined explicit and implicit algorithms for dynamic problems using the numerical manifold method

## X.L. Qu[1] and *G.W. Ma[1]

[1]School of Civil and Resource Engineering, The University of Western Australia, WA 6009, Australia

*Corresponding author: ma@civil.uwa.edu.au

## Abstract

The efficiency and accuracy are usually regarded as two general indices to check capability of a numerical method with respect to the time integration. The traditional numerical manifold method (NMM) employs implicit scheme to obtain high computational accuracy, but the efficiency is relatively low, especially when the iterations of contacts are involved. In this paper, the temporal coupled explicit-implicit (E-I) algorithm is proposed, in which the time integration schemes, transfer algorithm and contact algorithm are studied, respectively. A few numerical examples are simulated using the proposed coupled algorithms, in which one calibration example is studied with respect to the coupled temporal based on the cover system. The simulated results are well agreement with the implicit and explicit algorithms simulations, but the efficiency is improved evidently. It is predicted that the proposed couple E-I algorithm can be applied for larger scale engineering systems to combine the merits of both the implicit and the explicit algorithms of the NMM.

**Keywords:** Computational efficiency; Computational accuracy; Explicit algorithm; Implicit algorithm; Numerical manifold method.

## Introduction

The efficiency and accuracy are usually regarded as two indices to check capability of a numerical method in terms of time integration for dynamic problems. In general, there are two classes of time integration algorithms for dynamic problems: implicit and explicit (Gelin et al, 1995). Implicit algorithms possess such as the continuum-based finite element method (FEM) and discontinuum-based discontinuous deformation analysis (DDA), explicit algorithms such as finite difference method (FDM) and discrete element method (DEM). It is noted when more contact problems are involved in the discontinuum-based methods such as DDA and DEM, the efficiency is significantly declined. Thus, how to treat the contact problems balancing the efficiency and accuracy, an appropriate time integration algorithm is required.

In the present study, the numerical manifold method (NMM) is considered to combine the both time integration algorithms. The traditional NMM is originally proposed by Shi (1991, 1992). It employs the implicit time integration and open-close contact iteration for the simulations of complicated dynamic problems. Since the implicit scheme requires the assembling of the coupled global stiffness matrix for the governing equations, which may involve many thousand DOFs, especially when such more contact problems and nonlinear problems are encountered, the computational cost can be increased dramatically. Thus, the choice of an appropriate algorithm is essential to ensure efficiency and robustness of the numerical simulations, but the difficulty resides in being able to combine robustness, accuracy, stability and efficiency of the algorithms. The distinction between explicit and implicit where we have considered is that the explicit uses a diagonal mass matrix and the implicit applies a consistent inertia matrix (Liu and Belytschko, 1982). Then, a temporal

coupled E-I algorithm for the NMM based on the dual cover system is proposed, in which different time steps, time integration schemes are applied in temporal discretization. Then, some calibration examples and numerical simulations are studied to validate the coupled E-I algorithms.

## Basic Concept of the NMM and Its Dual Cover System

In the traditional NMM, one manifold element is generated through a set of overlapping covers, which is the distinct characteristic differs from other numerical methods. As shown in Figure 1(a), the mathematical cover system, which is united by six rectangle patches denoted by ①, ②, ③, ④, ⑤ and ⑥ respectively. The overlapping patches cover the whole material domain $\Omega$ without considering any physical properties, so any arbitrary shape of mathematical cover can be chosen. And then, physical covers can be obtained from these mathematical covers intersect with the physical domain $\Omega$, a manifold element can be produced as the common area of physical covers. Each small rectangle patch is termed as a mathematical cover (MC), denoted by $M_i$ (i= 1, 2, 3, …, 6). External boundary and internal joints or cracks may intersect one MC into several separate sub-patches, then each one within the material domain is termed as a physical cover (PC), denoted by $P_i^j$ ($j \in N$). As can be seen in Figure 1(b), material domain $\Omega$ is intersected by patch ① to generate one PC within its material domain, denoted by $P_1^1$. When the internal discontinuities (i.e. cracks or joints) are taken into accounted in the NMM, each discontinuous boundary is considered as one special material domain to form a new PC. If the crack passes through the whole patch within the material domain, two isolated PCs form by the crack surface just as $M_4$ and $M_6$, two separated PCs, denoted by $P_4^1$, $P_4^2$ based on $M_4$ and $P_6^1$, $P_6^2$ based on $M_6$, respectively. On the other case, when the crack cuts MC partially, only one PC forms within the material domain, which can be seen by $M_2$, $M_3$ and $M_5$, only one PC generates denoted by $P_2^1$, $P_3^1$ and $P_5^1$ respectively. Furthermore, the common area of several overlapping PCs is termed as a manifold element (ME).
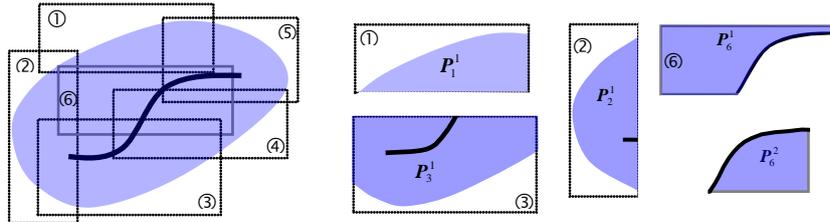


(a) General cover system in the NMM;   (b) Generation of physical covers for the NMM

**Figure 1. Cover system of the NMM.**

For convenience, a regularly structured mesh is employed in the NMM which is similar as that in the FEM. A regularly-patterned triangular mesh is employed, in which each MC is defined through six triangular elements sharing a common node (i.e. nodal star). Each cover has two degree of freedom is similar as node property in the FEM, each element formed by the overlapping of three neighboring hexagonal covers has six degree of freedom for the second order time integration. The mathematical mesh covers the whole physical domains form PC system. The common areas are formed by the neighboring three hexagonal MCs combined with the material domains. When the linear triangular element weight function is applied based on cover system, the global displacement function over a ME can be expressed as

$$u_e(x, \ y) = \sum_{i=1}^{3} \psi_i(x, \ y) U_i(x, \ y), \quad (x, \ y) \in \Omega_e \tag{1}$$

where $\psi_i(x, \ y)$ is the weight function over the three associated mathematical covers, $U_i(x, \ y) = \begin{Bmatrix} u_i(x, \ y) \\ v_i(x, \ y) \end{Bmatrix}$ is the displacement function on the three associated PCs. Here, it is the cover system makes the solution for both continuous and discontinuous problems practicability without any re-meshing technique used in the FEM.

## Temporary Coupled Explicit-Implicit Algorithm in the NMM

### The Coupled Explicit-Implicit Algorithm

For the different problems, there are two types of coupled approaches can be considered: implicit-explicit (E-I) algorithm and explicit-implicit (I-E) algorithm. When different approaches are employed, the different step time scale can be applied into the corresponding time integration scheme. To investigate the temporal couples algorithm, the E-I algorithm is taken into account in the present study. Furthermore, the Newmark-$\beta$ methods (Newmark, 1959) with two characteristic parameters $\beta$ and $\gamma$ for all sub-domains are assumed here. As is shown in Figure 2, initial diagonal mass matrix and force vector are constructed for the explicit algorithm (Ma and Qu, 2013), then the explicit central difference method, i.e. the Newmark method with the parameters $\beta_1 = 0$ and $\gamma_1 = 1/2$, is employed from the initial step time $t_0$ to $t_n$ at the step number $n$ to simulate the high frequency part of the dynamic problems. And then, the explicit integration algorithm switches to the implicit, in which the transfer algorithm is proposed in order to achieve the conservation of the kinematic energy from the explicit to implicit integration, and $D_E = D_I$, $v_E = v_I$ and $\sigma_E = \sigma_I$ are satisfied for the coupled E-I integration without the element and node partition. Thus, it is convenient to achieve in the programming. In the part of the implicit integration from step time $t_{n+1}$ to $t_{n+r}$, the constant acceleration method with the parameters $\beta_2 = 1/2$ and $\gamma_2 = 1$ is used in the implicit integration by the end of step $(n + r)$ for the low frequency and quasi-static problems. Continuing the explicit procedure, the initial inertial, stiffness matrix and force vector for the implicit integration are require to construct again as the difference items in the equations of motion. It is noted that different step time sizes are adopted before and after the transition in the couples E-I algorithm in terms of the numerical stability and accuracy, respectively. Normally, the step time size $\Delta t_I$ in the implicit algorithm is larger than $\Delta t_E$ in the explicit algorithm, which denotes $\Delta t_I = \alpha \cdot \Delta t_E$, $\alpha > 1$ is the coefficient to describe the scale between the implicit and explicit integrations. Sequentially, the transfer algorithm of the coupled E-I integration is exposed and discussed in the following section.
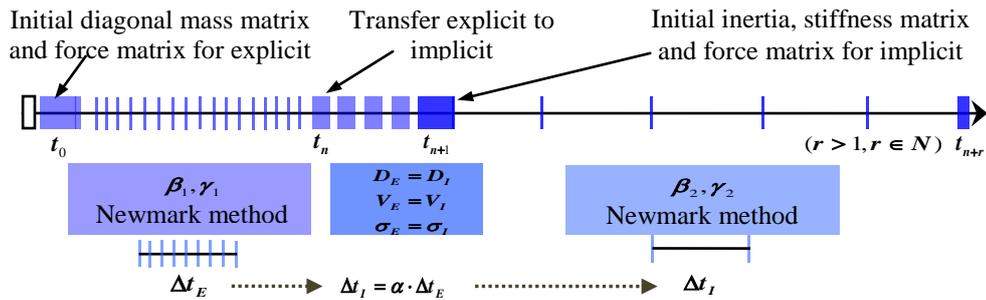


**Figure 2. Transfer algorithm from the explicit to implicit scheme.**

*Transfer Algorithm for the E-I Algorithm*

In the coupled E-I method, we employ the explicit algorithm to model motion of the system at the early stage, followed by the implicit algorithm to simulate the subsequent motions of the system. Thus, an explicit physical model in the NMM will be transferred to the implicit one at a certain time so that the coupled method is more efficient. In the transition, the geometric configurations, physical and mechanical parameters, and status, including stress state and velocities, are consistent and continue. Therefore, the transfer algorithm is required to satisfy the kinetic energy and potential energy conservation from the explicit integration to the implicit one, which can be represented as

$$\frac{1}{2}\sum_{i=1}^{n} M_i^E (v_x^{E\,2} + v_y^{E\,2}) = \frac{1}{2}\sum_{i=1}^{n} M_i^I (v_x^{I\,2} + v_y^{I\,2}) \qquad (2a)$$

$$\prod_e^E (\sigma_x^E, \sigma_y^E, \tau_{xy}^E) = \prod_e^I (\sigma_x^I, \sigma_y^I, \tau_{xy}^I) \qquad (2b)$$

where $M_i^E$ and $M_i^I$ are the $i$-th explicit and implicit element mass, respectively; $v_x^E$, $v_y^E$ and $v_x^I$, $v_y^I$ are the velocity components of an explicit element and implicit element in the $x$ and $y$ directions, respectively; $\prod_e^E (\sigma_x^E, \sigma_y^E, \tau_{xy}^E)$ and $\prod_e^I (\sigma_x^I, \sigma_y^I, \tau_{xy}^I)$ are the explicit and implicit element potential energy, in which $\sigma_x^E, \sigma_y^E, \tau_{xy}^E$ and $\sigma_x^I, \sigma_y^I, \tau_{xy}^I$ are stress components of the explicit and implicit elements respectively. Furthermore, equations of $M_i^E = M_i^I$, $v_x^E = v_x^I$, $v_y^E = v_y^I$, $\sigma_x^E = \sigma_x^I$, $\sigma_y^E = \sigma_y^I$, $\tau_{xy}^E = \tau_{xy}^I$ are satisfied in the transfer algorithm to ensure the parameters of the terms are consistent and the computation is continuous.

## Contact Algorithm for the Coupled Scheme

*Contact Force Calculation*

As previously mentioned, contact detection and contact force calculations are done by the NMM. Once contacts have been detected, a contact interaction algorithm is employed to evaluate contact forces between the contact elements. A thorough discussion and formulations of these approaches can be found in (Munjiza, 2004).

For a discrete block system involving $m$ elements, there are $N$ contact pairs have been detected to an element $i$ ($i = 1,2,\cdots m$). Here, we assume one element denoted by $j$ ($j = 1,2,\cdots N$) and $i$ are detected in contact state, $[K^c]$ between $i$ and $j$ can be expressed as

$$[K^c] = \begin{bmatrix} [K_{ii}^c] & [K_{ij}^c] \\ [K_{ji}^c] & [K_{jj}^c] \end{bmatrix} \qquad (3)$$

in which $[K_{ij}^c]$ is defined by the contact spring between the contact elements $i$ and $j$, and the value is zero if the elements $i$ and $j$ have no contact. Since each element is consisted by three associated PCs, thus the matrix $[K_{ij}^c]$ is a 6×6 sub-matrix and the derivation of the matrix $[K_{ij}^c]$ will be discussed in detail at the following section. It is noted that the displacement $\{D_{n+1}\}$ on the three associated PCs can be predicted using the Verlet algorithm by the previous step $n$. Then, contact forces associated with $[K_{ij}^c]$ on the contact element $i$ are assembled as

4

$$\{I_i^c\} = -\sum_{j=1}^{m}[K_{ij}^c]\cdot\{D_{i(r)}\}, \quad j=1,2,\cdots,N; r=1,2,3 \tag{4}$$

The total internal forces on the element $\boldsymbol{i}$ can be represented as

$$\{\tilde{I}_i\} = [K_{ii}^e]\cdot\{D_{i(r)}\} + \{I_i^c\} = \left([K_{ii}^e] + \sum_{j=1}^{N}[K_{ij}^c]\right)\cdot\{D_{i(r)}\}, \quad j=1,2,\cdots,N; \quad r=1,2,3 \tag{5}$$

in which $\{\tilde{I}_i\}$ is the element internal force vectors and $[K_{ii}^e]$ is the stiffness matrix of element. Since each element is formed by the three associated PCs, thus $\{\tilde{I}_i\}$ can be rewritten as

$$\{\tilde{I}_i\} = \begin{Bmatrix} \tilde{I}_{i(1)} \\ \tilde{I}_{i(2)} \\ \tilde{I}_{i(3)} \end{Bmatrix} \tag{6}$$

in which $\{\tilde{I}_{i(1)}\}$ maps the first PC associated the element, the subsequent $\{\tilde{I}_{i(2)}\}$ and $\{\tilde{I}_{i(3)}\}$ map the second and third PCs, respectively. Then, $\{\tilde{I}\}$ at each PC can be assembled by the associated $\{\tilde{I}_i\}$ on the cover system.

*Damping Algorithm*

It is noted that the explicit scheme employs dynamics method to solve the uncoupled equations, in which the generated kinetic energy can not be neglected. To the static or quasi-static problems, it requires the physical damping to adsorb the kinetic energy of the systems so that the systems achieve stable condition. As in reference (Cundall, 1982), we suggest an alternative scheme to simulate the damping, in which the damping force with the unbalance force or inertial force is in direction proportion, and the damping item of each MC in the NMM can be expressed as

$$\{F_d\} = -\zeta[M_e]\{\ddot{D}_e|_{t_0}\} \tag{7}$$

where $\{F_d\}$ is the damping force matrix, $\{\ddot{D}_e|_{t_0}\}$ is the element initial acceleration vector at the start of the time step. The total potential energy from the damping item is summered by each element, which can be written as

$$\Pi_d = \sum_e \zeta\{D_e\}^T[M_e]\{\ddot{D}_e|_{t_0}\} \tag{8}$$

Substituting Equation (8) using the variational principle, the equivalent damping force matrix can be described as

$$[F_d] = -\frac{\partial\Pi_d}{\partial\{D_e\}} = -\zeta[M]\{\ddot{D}_e|_{t_0}\} \tag{9}$$

which is a $6\times1$ matrix to produce external force item.

## Numerical Examples

*Calibration of the Coupled Algorithm*

In order to calibrate the proposed coupled E-I algorithm for the temporal problems, one Newmark sliding modelling of block sliding under input horizontal acceleration $\boldsymbol{a}_H$ is studied here. A block rests on an inclined plane is taken into account as a first approximation of the Newmark sliding model. The angle of the plane is $31.47^0$. And a sinusoidal seismic acceleration $\boldsymbol{a}_H$ is employed to impose the fixed point as expressed in Equation (10), where $\boldsymbol{g}$ is the gravity acceleration, $\boldsymbol{t}$ is the simulation duration for

the simulation. In this study, we assume the frictional angle $\phi = 30^0$, the total displacement of analytical solutions can be referred in (Newmark, 1959; An et al, 2011), then the simulated results of the proposed E-I NMM can be obtained as shown in Figure 3. It is noted that when the E-I algorithm is considered, the proposed transfer algorithm is employed from the explicit to implicit algorithm at the time of $t = 1s$, and the final results of the simulations are well agreement with the analytical solution.

$$a_H = \begin{cases} 0.1g \sin 4\pi t & t \le 1s \\ 0 & t > 1s \end{cases} \tag{10}$$
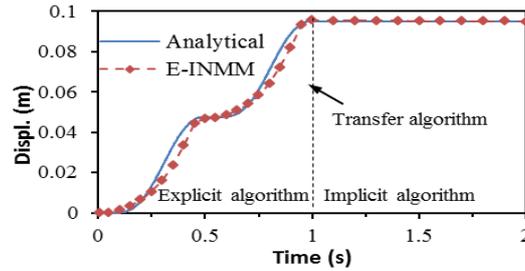


**Figure 3. Block displacement under horizontal ground acceleration.**
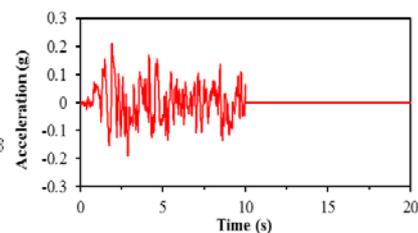
*Open-pit Mining Stability Analysis*

In this simulation, one open-pit mine slope modeling is assumed to study the stability using the proposed E-I algorithm. As shown in Figure 4, there are 9 layers denoted by 1# to 9# separate the whole modeling, in which we assume the layer 4# is the fracture zone constituted by many discontinuous joints. The inclined angle of the slope is 42° and drop is 120 m. In order to investigate the effect of the fracture zone to stability of the slope, two models of layer 4# are represented in Figure 5. Integrated Model considers the whole layer as one domain, on the other hand, Refined Model adds more joints into the layer to approach the realistic condition, in which a set of joints with orientation of $32.47^0$ are constructed as seen Figure 5 to simulate the fractured zone of the open-pit slope.
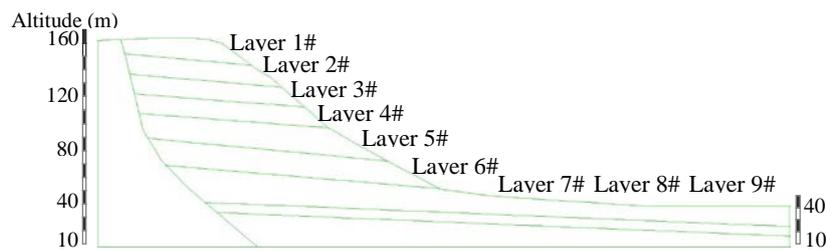


**Figure 4. Geology section of the open-pit mining.**
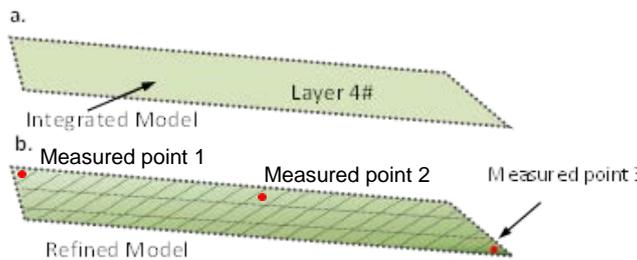


**Figure 5 Study model of the layer 4#.**      **Figure 6 Input seism acceleration.**

6

Traditional methods apply to the slope stability analysis is to determine the factor of stability (FoS) of the slope using the limit equilibrium method (LEM) without considering the effect of the dynamic loading with time history (i.e. seismic loading, blasting loading, etc). Here, the FoS is computed using the LEM to the integrated model, FoS can be determined as 1.436 and 2.182 by cases of $10^0$ and $15^0$ of joint frictional angle. To further investigate the stability of the slope under the earthquake, a stochastic horizontal seismic acceleration with maximum value of 0.2g is applied as shown in Figure 6.The detailed of physical parameters such as unit weight is 26.0 kN/m3, Young's modulus is 1.0 GPa, Possion's ratio is 0.2, Joint normal stiffness is 1.0 GPa and Joint shear stiffness is 0.5 GPa, respectively.

To investigate the instability of the fracture zone under earthquake loading, the measure points selected in the fracture zone and the displacements of them at both cases of $\phi=10^0$ and $\phi=15^0$ are presented in Figure 7 and 8, respectively. It is verified that the proposed E-INMM satisfies the computational accuracy comparing with the original NMM. We can find that the slope is instable at the case of $\phi=10^0$ whether static or dynamic states, but the slope approaches to be stable after the seismic loading at the case of $\phi=15^0$. Thus, the fractured zone should be taken into account to the design of the open-pit slope to improve the stability of slope.
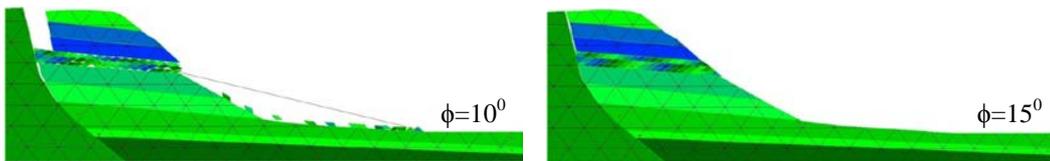


**Figure 7. Simulations for Refined Model (Total time: 20s).**



(a) $\phi=10^0$;        (b) $\phi=15^0$.
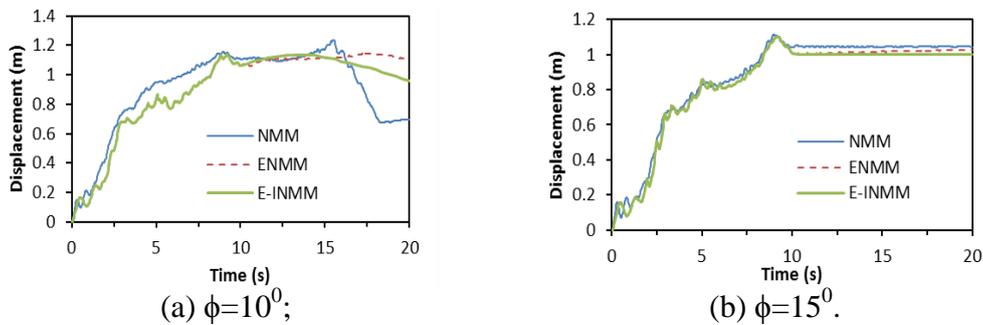
**Figure 8. Measured point 1 in the Refined Model.**

With respect to the efficiency of the proposed algorithms, CPU time is taken into consideration to check the computational cost of the algorithms. All three algorithms are run on the same computer with the system configuration: processor speed = 4.0 GHz and RAM = 4.0 GB. As represented in Table 1, the proposed E-I algorithm is more efficient comparing the explicit and implicit algorithms in the refined model with both cases of $\phi=10^0$ and $\phi=15^0$. In particular, E-I algorithm can be considered as one computational criteria for the large scale engineering as it combines the merits of both the explicit and implicit algorithms in terms of accuracy and efficiency of the computations dramatically.

**Table 1. CPU cost for the different cases (hr.).**

| Study Case | 10° | | | 15° | | |
|---|---|---|---|---|---|---|
| | $CPU^I$ | $CPU^E$ | $CPU^{E-I}$ | $CPU^I$ | $CPU^E$ | $CPU^{E-I}$ |
| Refined Model | 1.467 | 1.376 | 0.882 | 1.816 | 1.515 | 0.911 |

## Conclusions

The temporal coupled explicit and implicit algorithm for the numerical manifold method (NMM) is proposed in this paper. The time integration schemes, transfer algorithm, contact algorithm and damping algorithm are studied in the temporal coupled E-I algorithm to combine both merits of the explicit and implicit algorithms in terms of efficiency and accuracy. Then, some numerical examples are simulated using the proposed coupled algorithms, in which one calibration example is studied with respect to the coupled temporal based on the dual cover system. One numerical example of open-pit slope seismic stability analysis using the coupled E-I algorithm is investigated as well. The simulated results are well agreement with the implicit and explicit algorithms simulations, but the efficiency is improved evidently. It is predicted that the couple E-I algorithm proposed in the present paper can be applied into larger scales engineering systems to combine the merits of both the implicit and explicit algorithms in the NMM.

## References

An, X. M., Ning, Y. J., Ma, G. W. and Zhao, Z. Y. (2011). Seismic stability analysis of rock slopes using the numerical manifold method. *12th International Congress on Rock Mechanics, Beijing*, pp, 693-698.

Cundall, P. A. (1982), Adaptive density-scaling for time-explicit calculations. *Proceedings of the 4th international conference on numerical methods in geomechancs, Rotterdam*: A. A. Balkema, pp, 23-26.

Gelin, J. C., Boulmance, L. and Boisse, P. (1995), Quasi-static implicit and transient explicit analyses of sheet-metal forming using a c0 three-nodes shell element. *Journal of material processing technology*, pp. 395-409.

Liu, W. K. and Belytschko, T. (1982), Mixed-time implicit-explicit finite elements for transient analysis. Journal of computers and structures, Vol.15 (4), pp, 445-450.

Ma, G. W. and Qu, X. L. (2013), An explicit version of the numerical manifold method and its applications. *Proc. Eleventh Int. Conf. Analysis of Discontinuous Deformation (ICADD-11), Fukuoka Japan*, pp. 315-321.

Munjiza, A. (2004), The combined Finite-Discrete Element Method. John Wiley & Sons Ltd.

Newmark, N.M. (1959), A method of computation for structural dynamics. *Journal of Engineering and Mechanics Division*, 85, pp. 67-94.

Shi, G. H. (1988), Discontinuous deformation analysis: A new numerical method for the static and dynamic of block system. *PhD dissertation*, Dep. of Civ. Engrg., University of California, Berkeley, Calif.

Shi, G. H. (1991), Manifold method of material analysis. In: *Transactions of the 9th army conference on applied mathematics and computing, Minneapolis, Minnesota*, pp. 57- 76.

Shi, G. H. (1992), Modeling rock joints and blocks by manifold method. In: *Proceedings of the 33rd US rock mechanics symposium, Santa Fe, New Mexico*, pp. 639- 648.